X-band Cascode LNA with Bias-invariant Noise Figure using 0.15 µm GaN-on-SiC Technology

Muhammad Imran Nawaz
Nanotechnology Research Center (NANOTAM)
Department of Electrical and Electronics Engineering
Bilkent University
Ankara, Turkey
imran.nawaz@bilkent.edu.tr

Yunus Erdem Aras
Nanotechnology Research Center (NANOTAM)
Department of Electrical and Electronics Engineering
Bilkent University
Ankara, Turkey
erdem.aras@bilkent.edu.tr

Salahuddin Zafar
Nanotechnology Research Center (NANOTAM)
Department of Electrical and Electronics Engineering
Bilkent University
Ankara, Turkey
salahuddin.zafar@bilkent.edu.tr

Busra Cankaya Akoglu
Nanotechnology Research Center (NANOTAM)
Ankara, Turkey
busra.cankaya@bilkent.edu.tr

Gizem Tendurus
Nanotechnology Research Center (NANOTAM)
Ankara, Turkey
gizem.tendurus@bilkent.edu.tr

Ekmel Ozbay
Nanotechnology Research Center (NANOTAM)
Department of Electrical and Electronics Engineering
Bilkent University
Ankara, Turkey
ozbay@bilkent.edu.tr

***Abstract*— Cascode HEMTs exhibit better stability and broad bandwidths performance as compared with common source HEMTs. This paper presents the design of a single stage broadband low noise amplifier based upon 0.15 um GaN HEMT technology in the frequency range of 8 – 12 GHz. Cascode HEMT with inductive source degeneration is utilized. All the design work is done using PathWave Advanced Design System. The LNA provides 9.5 to 10.6 dB with input return loss better than 10 dB and output return loss better than 8 dB in the whole band. The noise figure of the amplifier is below 1.9 dB. The linearity parameters P$_1$dB and OIP3 are greater than equal to 16 dBm and 28 dBm respectively within operating bandwidth. The noise figure of the amplifier is fairly constant over 30 mA to 60 mA bias currents and 9 V – 18 V operating bias voltage. This is a unique finding which is being reported for the first time to the best of authors' knowledge.**

Keywords—GaN HEMT, low noise amplifier, X-band, Cascode, source degeneration, bias-invariant

I. INTRODUCTION

GaN technology is the first choice of the microwave community for the design of transmitter, receiver, and transceiver circuits. GaN has a wide bandgap and high breakdown nature. Moreover, GaN-on-SiC provides better thermal characteristics. Due to these advantages, a lot of work is done and reported on GaN based power amplifiers. GaN HEMT technology provides faster and robust low noise amplifiers with high survivability as compared with GaAs counterparts, thus eliminating the need for limiter after the receive antenna in the front-end assembly. Efforts are being put to design broadband low noise amplifiers over the past few years [1].

Performance of GaN HEMT low noise amplifier (LNA) depends upon HEMT configuration i.e. common source (CS), common gate, or cascode. CS HEMTs are better among all in terms of providing simultaneous noise and input impedance match [2–4]. Cascode HEMTs provide better linearity, stability, wider bandwidth, and higher gain [5–8].

In this paper, the effects of CS and cascode configurations are jointly investigated. We have designed an MMIC LNA using cascode GaN HEMT operating at X-band. The amplifier has fairly constant noise figure (NF) irrespective of bias current and voltage change over a wide range reported for the first time to the best of authors' knowledge. Rest of the paper is organized as follows: Section II discusses simulation and design; fabrication and measurements results are included in section III, while conclusion is made in section IV.

II. MMIC DESIGN

A. HEMT Selection

The selection of HEMT is the first step in the design of an MMIC. Source degenerated (SD) HEMTs are better than CS HEMTs as they provide simultaneous noise and input impedance match [2]. Cascode HEMTs can inherently provide broad bandwidths performances without the need for any feedback network. Source degenerated (SD) versions comprising CS and cascode are the focus of our current study.

We have compared noise, available gain and output power parameters of CS 4x50 um HEMT with 4x50 um cascode HEMT from in-house 0.15 um AlGaN/GaN on SiC HEMT fabrication process. Fig. 1 shows that maximum available gain (MAG) of cascode HEMT is higher than CS HEMT e.g. MAG is 18.9 dB for cascode HEMT at 10GHz while for CS HEMT it is 10.7 dB. On the other hand, minimum noise figure (NF$_{min}$) of CS HEMT is better than that of cascode HEMT e.g. NF$_{min}$ is 0.7 dB for CS HEMT while for cascode it is 1.0 dB at 10 GHz. Fig. 2 and 3 show load-pull contours of CS and cascode HEMTs. The optimum power available from cascode HEMTs is 22 dBm, this is higher than the power available from CS HEMT which is 20.7 dBm at 10 GHz. Therefore, due to better MAG, quite reasonable NF$_{min}$, and higher output power, we preferred cascode HEMT over CS HEMT for MMIC design.

B. Circuit Simulations

Our aim is to design a single stage LNA operating in the frequency range of 8 – 12 GHz. From small signal scattering parameters [S] of chosen HEMT, stability analysis is performed and it is made unconditionally stable over the entire measurement range (800 MHz to 18 GHz) through a series combination of L-C and R-C networks on the gate (Lib-Cib, Ris-Cib2) and drain (Lob-Ros-Cob1, Ros2-Cob2) bias lines as

2022 Microwave Mediterranean Symposium (MMS) | 978-1-6654-7110-7/22/$31.00 ©2022 IEEE | DOI: 10.1109/MMS55062.2022.9825619

shown in Fig 4. The 1 kΩ “Ris” resistor is dual purpose, it is providing stability as well as increases device survivability by making gate-source voltage more negative under application of high input signal [9]. The resistor values Ros1 and Ros2 on the drain side are comparatively small i.e. just 10 Ω and 30 Ω respectively. The large 17 pF capacitances Cib2 and Cob2 are providing stability especially, at low frequencies.

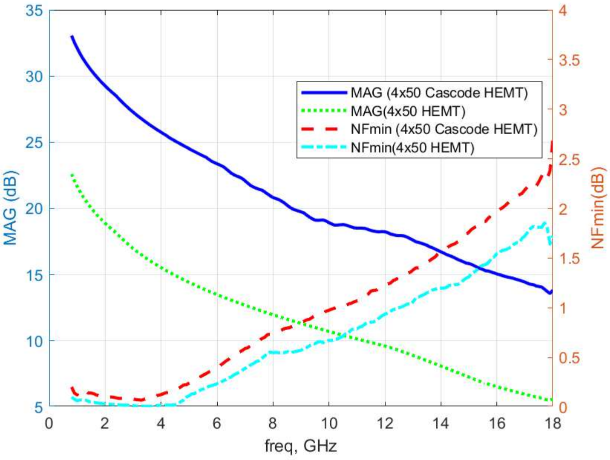

Fig. 1. NF_{min} and MAG comparison of 4x50 um CS and cascode HEMTs

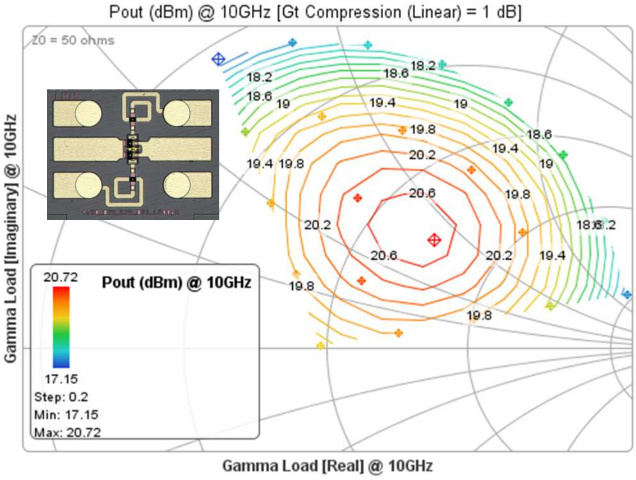

Fig. 2. Load pull contours of 4x50 um CS HEMT

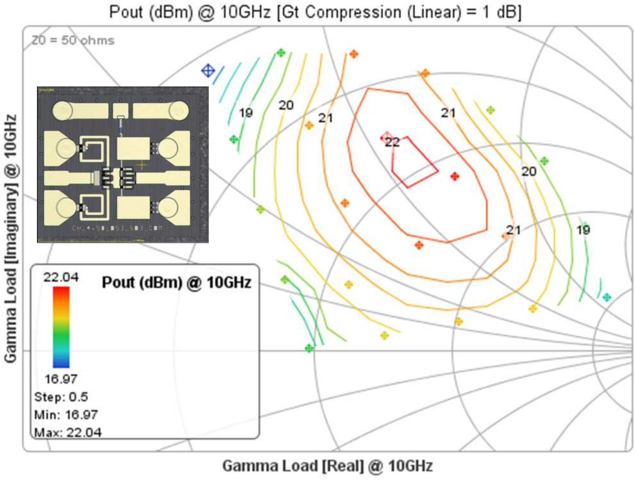

Fig. 3. Load pull contours of 4x50 um cascode HEMT

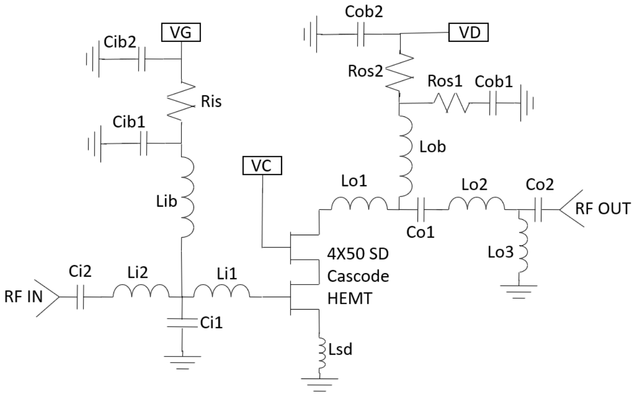

Fig. 4. Circuit schematic of proposed cascode LNA

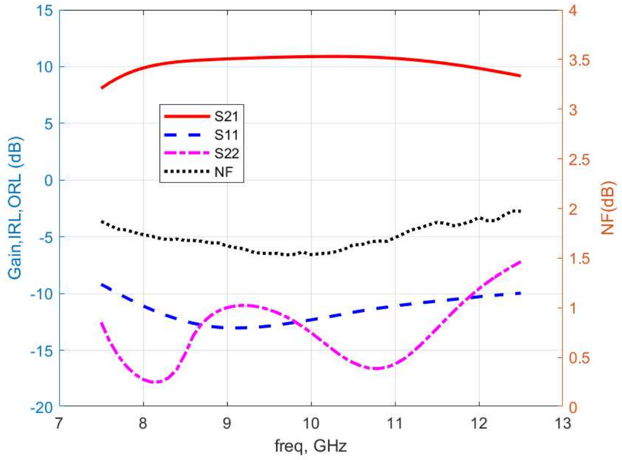

Fig. 5. EM simulation results of proposed cascode LNA

With stability achieved, optimum source impedance for NF_{min} is determined and input impedance matching network (IMN) is designed using Li1-Ci1-Li2 T-network topology. Output is conjugately matched to the S22 obtained by incorporating HEMT, stability network, and IMN altogether. In this case, Lo2-Lo3-Co2 T-network with series Lo1-Co1 is determined as output matching network (OMN). It is to be mentioned that 4x50 HEMT is a small periphery device and S12 (feedback from the output) is significant which disturbs our optimum noise impedance point and hence NF. Therefore, optimization of the whole circuit is done using optimization routines by setting noise figure, gain, input return loss (IRL), and output return loss (ORL) goals.

Fig. 5 shows the Electromagnetic (EM) simulation results of the MMIC amplifier. The broadband response is obtained from 8 GHz – 12 GHz. Gain is 10 dB with values of 9.9 dB and 9.8 dB at band edges. However, the gain flatness is ± 0.5 dB in the whole band. Both IRL and ORL are better than 10 dB with exception of 9.6 dB ORL at 12 GHz. NF is below 2 dB with particular values of 1.7, 1.5, and 1.9 dB at 8, 10, and 11 GHz.

III. FABRICATION AND MEASUREMENTS

Fig. 6 shows the layout of MMIC. Circular vias are utilized for grounding purpose. Long inductive transmission lines are meandered to minimize the overall area. Spacing between any two adjacent lines is maintained to be 70 um at least to reduce EM coupling effects. DC and RF pads are included for measurement and interconnection purposes. Total size is 2.8 mm x 1.5 mm. Design is fabricated using NANOTAM's in-house GaN HEMT technology on a 3-inch SiC substrate.

Small signal, large signal, and noise measurements are done on the fabricated device with a typical continuous bias of 12 V and 50 mA. Control voltage is set to

$$VC = \frac{VD}{2} - |VG| \qquad (1)$$

Where VD and VG are drain and gate voltages respectively.

Fig. 7 shows small signal measured response of the MMIC. Gain is 10.6 dB at center frequency while at edges it is 9.5 dB and 9.6 dB. These values are close to simulated values of 10.9 dB, 9.9 dB and 9.8 dB respectively. IRL is 10.2 dB and 12.1 dB at band edges which is slightly shifted towards right as corresponding simulated values are 11 dB and 10.2 dB due to fabrication tolerances. ORL is 15.7 dB and 8.4 dB which is lower than simulated 17.6 dB and 9.6 dB at 8 GHz and 12 GHz respectively. Besides negligible differences, overall measured results are in good agreement with the simulations.

Noise performance of the MMIC is measured under different bias voltages and currents. Fig. 8 shows the noise figure for fixed 12 V with variable bias currents. For a typical bias current of 50 mA, NF is 1.8 dB at 8 GHz, 1.9 dB at 12 GHz, and 1.7 dB at 10 GHz which are close to corresponding simulated values of 1.7 dB, 1.9 dB, and 1.5 dB. NF is raised to 0.2 dB in the mid-band, however, the overall NF is below 2 dB as in the simulated one in the whole band. It is noticeable that the NF is almost independent of bias currents since we varied current from 30 mA to 60 mA, overall NF is still below 2 dB and curves are overlapping each other showing that there is not much difference. Moreover, we also investigated the effect of different bias voltages of 9,12,15, and 18 volts as shown in Fig. 9. The bias current chosen is 30 mA. It is seen that the overall NF is still below 2 dB. There is no significant difference in the value of NF from one bias voltage to another. This can be a novel important conclusion that is specific to cascode HEMT topology ever reported to the best of the authors' knowledge. This means that cascode GaN HEMTs based low noise amplifiers can provide large flexibility in bias voltages and currents in terms of NF.

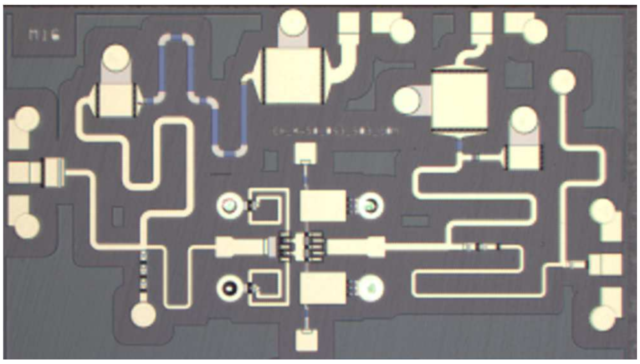

Fig. 6. Fabricated cascode LNA

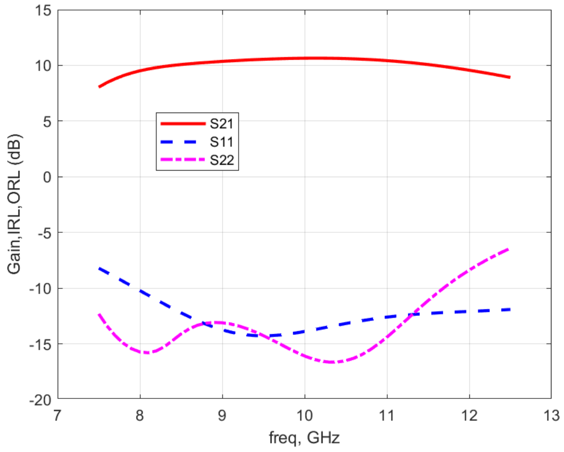

Fig. 7. Small signal measurement results of proposed cascode LNA

Large signal measurements of the device are also performed to determine P_1dB and OIP3. The P_1dB of MMIC is above 16 dBm measured at three different frequencies of 8,10, and 11GHz with the highest value of 18 dBm at 10 GHz as shown in Fig. 10. OPI3 is measured using two-tone test with carrier spacing of 10 MHz. The measured value is ≥ 28 dBm.

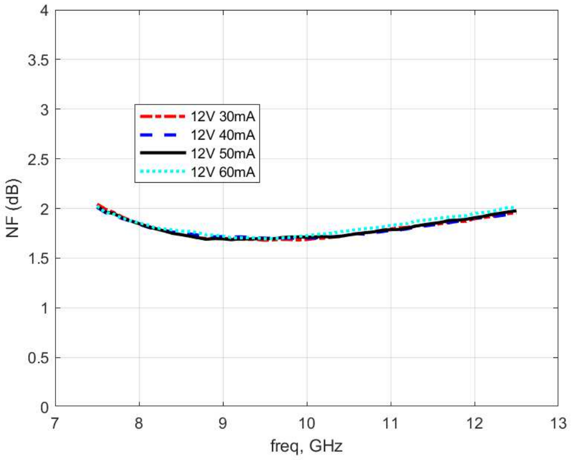

Fig. 8. NF measurement results under different bias currents

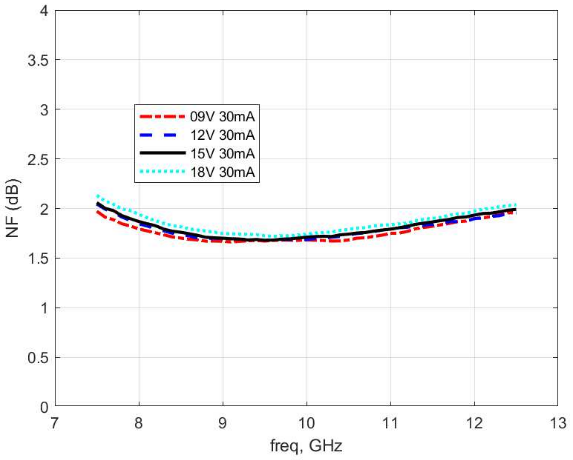

Fig. 9. NF measurement results under different bias voltages

Table 1. Comparison of proposed cascode LNA with reported data in X-band

Ref.	Freq (GHz)	IRL (dB)	ORL (dB)	Gain (dB)	NF (dB)	Gain Flatness (dB)	OIP3 (dBm)	Gate length Lg (um)	HEMT Configuration
[5]	9 – 11	< 11	< 4	> 13.5	< 2.2	≤ 0.5dB	≥ 29.5	0.15	Cascode
[10]	8 – 11	< 9.8	< 12.8	> 8	< 1.4*	≤ 1.4dB	-	0.15	CS
[11]	9 – 11	< 10	-	> 13.5	< 1.5	≤ 0.75dB	≥ 28	0.09	Cascode
This work	**8 – 12**	**< 10**	< 8.4	> 9.5	**< 1.9**	**≤ 0.5dB**	≥ 28	0.15	Cascode

* simulated result

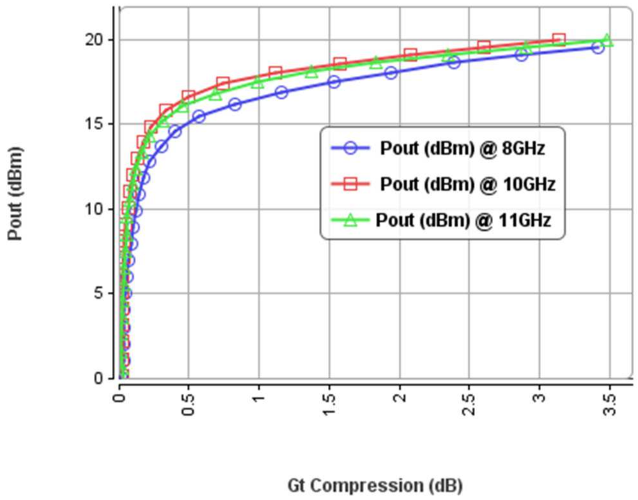

Fig. 10. Large signal measurements (P_1dB) of proposed cascode LNA

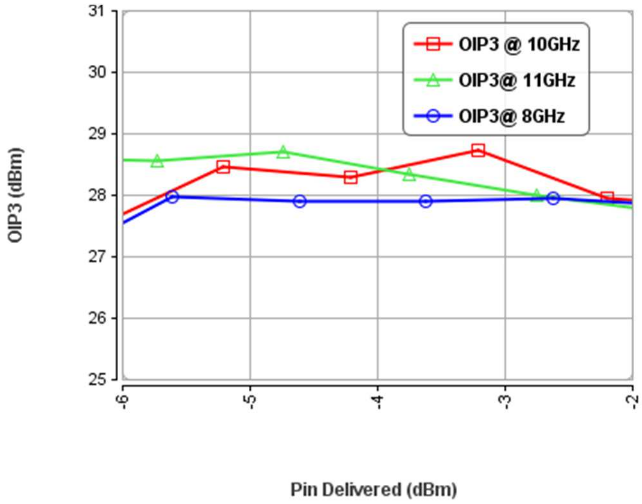

Fig. 11. OIP3 measurements of proposed cascode LNA

Finally, this work is compared with already reported single stage cascode and CS HEMT configurations based low noise amplifiers in X-band. The bandwidth of the designed amplifier is 1 – 2 GHz higher than others. Secondly, gain flatness is either comparable or better than reported ones. IRL is also comparable while OIP3 is close to reported values.

IV. CONCLUSION

We have described the design of a low noise amplifier covering the complete X-band based on Cascode source degenerated HEMT configuration. This configuration provides quite wide bandwidth with good input and output return losses. The measured results are in good agreement with simulated ones. The noise figure of the amplifier is below 1.9 dB which is quite stable and insensitive to change of bias current and bias voltages. This amplifier can be used for electronic systems operating in the X-band e.g. radars, satellites, etc.

ACKNOWLEDGMENT

The authors would like to thank fabrication and measurement teams from Nanotechnology Research Center (NANOTAM) in particular Mr. Dogan Yilmaz, Mr. Emirhan Urfali and Mr. Mahmut Can Soydan.

REFERENCES

[1] M. Rudolph, "GaN HEMTs for low-noise amplification — status and challenges," 2017 Integrated Nonlinear Microwave and Millimetre-wave Circuits Workshop (INMMiC), 2017, pp. 1-4.

[2] Sabzi, M., and Ali Medi. "Analysis and design of multi-stage wideband LNA using simultaneously noise and impedance matching method." Microelectronics Journal 86 (2019): pp. 97-104.

[3] S. Zafar, S. Osmanoglu, B. Cankaya, A. Kashif and E. Ozbay, "GaN-on-SiC LNA for UHF and L-Band," 2019 European Microwave Conference in Central Europe (EuMCE), 2019, pp. 95-98.

[4] M. Tasci, O. Sen, U. Ozipek and E. Ozbay, "GaN HEMT Based MMIC High Gain Low-Noise Amplifiers for S-Band Applications," 2019 IEEE 19th Mediterranean Microwave Symposium (MMS), 2019, pp. 1-5.

[5] K. W. Kobayashi, C. Campbell, C. Lee, J. Gallagher, J. Shust and A. Botelho, "A reconfigurable S-/X-band GaN cascode LNA MMIC," 2017 IEEE Compound Semiconductor Integrated Circuit Symposium (CSICS), 2017, pp. 1-4.

[6] A. H. Jarndal and A. M. Bassal, "A broadband hybrid GaN cascode low noise amplifier for WiMax applications," 2018 3rd International Conference on Microwave and Photonics (ICMAP), 2018, pp. 1-2.

[7] L. M, N. H and K. S, "Compact X Band MMIC Low Noise Amplifier for Radar Applications," 2020 IEEE International Conference for Innovation in Technology (INOCON), 2020, pp. 1-4.

[8] A. H. Jarndal and A. M. Bassal, "A broadband hybrid GaN cascode low noise amplifier for WiMax applications," 2018 3rd International Conference on Microwave and Photonics (ICMAP), 2018, pp. 1-2.

[9] M. Rudolph et al., "Analysis of the Survivability of GaN Low-Noise Amplifiers," in IEEE Transactions on Microwave Theory and Techniques, vol. 55, no. 1, pp. 37-43, Jan. 2007.

[10] S. Zafar et al., "GaN based LNA MMICs for X-Band Applications," 2020 17th International Bhurban Conference on Applied Sciences and Technology (IBCAST), 2020, pp. 699-702.

[11] K. W. Kobayashi, V. Kumar, C. Campbell, S. Chen, Y. Cao and J. Jimenez, "Robust-5W Reconfigurable S/X-band GaN LNA using a 90nm T-gate GaN HEMT Technology," 2020 IEEE BiCMOS and Compound Semiconductor Integrated Circuits and Technology Symposium (BCICTS), 2020, pp. 1-4.